Physics of Plasmas

Nonlinear structures of lower-hybrid waves driven by the ion beam

Cite as: Phys. Plasmas **25**, 061209 (2018); https://doi.org/10.1063/1.5024237
Submitted: 30 January 2018 . Accepted: 29 May 2018 . Published Online: 22 June 2018

O. Koshkarov, A. I. Smolyakov, A. Kapulkin, Y. Raitses, and I. Kaganovich

Nonlinear structures of lower-hybrid waves driven by the ion beam

O. Koshkarov,[1,2,a)] A. I. Smolyakov,[2] A. Kapulkin,[3] Y. Raitses,[4] and I. Kaganovich[4]
[1]*T-5 Applied Mathematics and Plasma Physics Group, Los Alamos National Laboratory, Los Alamos, New Mexico 87545, USA*
[2]*Department of Physics and Engineering Physics, University of Saskatchewan, Saskatoon, Saskatchewan S7N 5E2, Canada*
[3]*Asher Space Research Institute, Technion (Israel Institute of Technology), Haifa, Israel*
[4]*Princeton Plasma Physics Laboratory, Princeton, New Jersey 08543, USA*

(Received 30 January 2018; accepted 29 May 2018; published online 22 June 2018)

The lower-hybrid waves can be driven unstable by the transverse ion beam in a partially magnetized plasma of a finite length. This instability mechanism, which relies on the presence of fixed potential boundary conditions, is of particular relevance to axially propagating modes in a Hall effect thruster. The linear and nonlinear regimes of this instability are studied here with numerical simulations. In the linear regime, our results agree with analytical and numerical eigenvalue analysis conducted by Kapulkin and Behar [IEEE Trans. Plasma Sci. **43**, 64 (2015)]. It is shown that in nonlinear regimes, the mode saturation results in coherent nonlinear structures. For the aperiodic instability [with $Re(\omega) = 0$—odd Pierce zones], the unstable eigen-function saturates into new stationary nonlinear equilibrium. In the case of oscillatory instability [$Re(\omega) \neq 0$—even Pierce zones], the instability results in the nonlinear oscillating standing wave. It is also shown that finite Larmor radius effects stabilize instability for parameters corresponding to a large number of Pierce zones, and therefore, only few first zones remain relevant. *Published by AIP Publishing.*
https://doi.org/10.1063/1.5024237

I. INTRODUCTION

Partially magnetized plasmas where electrons undergo fast gyro rotation, while ion dynamics are not significantly affected by the magnetic field, are common in many applications such as Hall-effect thrusters, magnetrons, and some regions of the ionosphere. This is the typical regime of the so-called $\mathbf{E} \times \mathbf{B}$ discharges, e.g., Hall thrusters for electric propulsion[2] and magnetrons.[3] Plasmas in such discharges are typically strongly turbulent, exhibit fluctuations of different temporal and spatial scales, and are characterized by anomalous current. Understanding of the nature and sources of these instabilities is an area of active research.

Local plasma gradients, such as in density, temperature, and magnetic field, are usually identified as sources of free energy, resulting in plasma instabilities and turbulence. These instabilities referred as drift instabilities have also been studied in partially magnetized plasmas.[4,5]

In the short wavelength limit, linear plasma dynamics is local and is formally described by linear partial differential equations (PDEs) with constant coefficients. However, when the mode wavelength is of the order of the system size or/and plasma equilibrium length scale, the wave dynamics becomes nonlocal. In particular, the role of boundary conditions becomes non-trivial, which may result in new nonlocal instability mechanisms. An example is the Pierce instability,[6] in which plasma flow in a finite length plasma with boundaries results in the instability, whereas in the periodic (infinite) plasmas, such flow would only lead to a trivial Doppler frequency shift. Such instabilities driven by boundary effects for ion sound type waves and electric charge waves in non-compensated diodes were studied in a number of experimental and theoretical works (see, e.g., Refs. 7–10 and references therein).

It was recently shown that the lower-hybrid waves can be driven by the transverse ion-beam in a finite length system via the mechanism similar to the Pierce instability in which the role of boundaries is crucial for the instability.[1] The present paper is devoted to the investigation of nonlinear regimes of this instability and its consequences.

The lower-hybrid mode is among the most important modes in partially magnetized plasmas relevant to electric propulsion.[5] The nonlinear dynamics of resistive lower hybrid instability induced by ions flow was recently studied in Ref. 11. This instability is relevant to axial (along the direction of the electric field) modes of $\mathbf{E} \times \mathbf{B}$ plasma discharges such as Hall-effect thrusters and magnetrons.[12] In the previous work,[11] it was shown that numerical simulations confirm the predictions of the local theory for the most unstable modes in periodic geometry. It was also shown that in the nonlinear stage, the highly localized (cnoidal type) wave structures are formed. The mechanism of this instability is local and related to the phase shift between the perturbations of the electron and ion currents. The electron current is supported by plasma conductivity across the magnetic field which may have classical (collisional) or anomalous (turbulent and/or wall conductivity) nature. At the same time, the ion current is due to the inertial response to the electric field and thus is shifted in phase due to the Doppler effect. It was shown in Ref. 1 that lower hybrid waves can be driven unstable by the ion beam due to boundary effects. The wavelengths of those modes usually are of the order of the system length, and therefore, the dynamics is highly nonlocal.

[a)]Electronic mail: koshkarov.alexandr@usask.ca

Both of these instability mechanisms are relevant to the axially propagating modes in the Hall thruster (e.g., breathing modes) which are known to significantly affect the ion thrust.[13,14] Modes exited by boundary effects are highly nonlocal in comparison to modes induced by the resistive electron current. Therefore, the nonlinear dynamics is expected to be different. The objective of this work is to investigate linear and nonlinear stages of the instability described in Ref. 1 when the "boundary" effect dominates over collisional instability, in order to see the difference in dynamics and ensuing nonlinear structures in their "pure" form. We note that parameters of various experiments (collisionality and level anomalous transport) vary widely with respect to the dominance of one or another effect. The investigation of the dissipative and boundary effects together is left for future publications. In order to study nonlinear dynamics, the nonlinear simulations were performed with the BOUT++ plasma fluid simulation framework.[15]

This paper is organized as follows: In Sec. II, the nonlinear two-fluid model for low-hybrid instability is discussed. The results for linear instability from Ref. 1 are recovered in Sec. III. In Sec. IV, the numerical solution to the full nonlinear model is obtained. The effect of the finite Larmor radius on the linear instability is analyzed in Sec. V. Finally, the conclusions and discussions are in Sec. VI.

II. ONE DIMENSIONAL MODEL FOR LOWER-HYBRID WAVES IN PARTIALLY MAGNETIZED PLASMAS

In this section, we introduce the one-dimensional axial fluid model for partially magnetized plasmas used in Ref. 1 to describe the ion beam instability in bound plasma systems. The dynamics of unmagnetized ions is considered along the constant equilibrium electric field in the x-direction, while magnetized electrons (i.e., equilibrium electric and magnetic fields are perpendicular) assumed to have zero collisional mobility along this direction and quasi-neutrality are supported by electron polarization drift.

Following the derivation in Ref. 1, two-fluid approximation with unmagnetized cold singly ionized ions and magnetized cold electrons is used. One dimensional mass and momentum conservation equations for ions written for perturbations around equilibrium yield

$$\partial_t n + n_0\partial_x v + v_0\partial_x n + v\partial_x n_0 + n\partial_x v_0 + \partial_x(nv) = 0, \quad (1)$$

$$\partial_t v + v_0\partial_x v + v\partial_x v + v\partial_x v_0 + \frac{e}{M}\partial_x\phi = 0, \quad (2)$$

with equilibrium profiles

$$n_0 = \frac{n_{00}v_{00}}{v_0}, \quad v_0 = \sqrt{v_{00}^2 + \frac{2eE_0}{M}x}, \quad (3)$$

where ∂_t, ∂_x are the time and space derivatives, respectively; $n_0 = n_0(x), v_0 = v_0(x)$ are the equilibrium profiles of ion density and velocity, respectively; $n_{00} = n_0(0)$ and $v_{00} = v_0(0)$; n and v are the perturbed ion density and velocity, respectively; ϕ is an electrostatic potential perturbation; E_0 is a constant electric field along the x direction; $x \in [0, L]$ is a spatial domain of length L; e is an absolute value of an electron charge; and M is an ion mass. We note that the assumption of constant electric field $E_0 = const$ implies the equilibrium electrostatic potential to grow as $\phi_0 \sim x$.

In the absence of collisions and in the strong magnetic field, the electron inertial response is compensated by the polarization drift in the axial direction. The electron dynamics can be recovered from the mass conservation equation

$$\partial_t n + n_0\partial_x u + u\partial_x n_0 = 0, \quad (4)$$

where the electron velocity perturbation in the axial direction (u) is supported by polarization drift (in the main order of strong magnetic field expansion $\partial_t \ll \omega_{ce}$)

$$u = \frac{e}{m\omega_{ce}^2}\partial_t\partial_x\phi, \quad (5)$$

where m is an electron mass and ω_{ce} is an electron cyclotron frequency. Hence, the final electron equation reads

$$\partial_x^2\phi + \frac{1}{n_0}\partial_x n_0\partial_x\phi + \frac{m\omega_{ce}^2}{en_0}n = 0, \quad (6)$$

where the time derivative was removed (integrated out). In principle, the right hand side of Eq. (6) is a function of time; however, it can be chosen to be zero for all relevant physical initial conditions (this assumption was verified numerically). This equation can also be derived from a general nonlinear equation,[5] from which all nonlinear terms disappear in one dimensional geometry considered here.

The system is closed with standard[1,6] boundary conditions which correspond to zero perturbation at the emanating left boundary ($x = 0$) and open boundary at the right ($x = L$)

$$\phi(0) = \phi(L) = n(0) = v(0) = 0. \quad (7)$$

III. LINEAR INSTABILITY

In the linear approximation, the system of Eqs. (1)–(6) reduces to

$$\partial_t n + n_0\partial_x v + v_0\partial_x n + v\partial_x n_0 + n\partial_x v_0 = 0, \quad (8)$$

$$\partial_t v + v_0\partial_x v + v\partial_x v_0 + \frac{e}{M}\partial_x\phi = 0, \quad (9)$$

$$\partial_x^2\phi + \frac{1}{n_0}\partial_x n_0\partial_x\phi + \frac{m\omega_{ce}^2}{en_0}n = 0. \quad (10)$$

Note that in the local approximation, when equilibrium profiles can be considered constant ($\partial_x n_0 \approx \partial_x v_0 \approx 0$), the system (8)–(10) is reduces to Pierce equations[6] which can be solved analytically.

As was shown in Ref. 1, the boundary conditions (7) make the system of Eqs. (8)–(10) unstable similar to the Pierce instability. The growth rate of this system was extensively studied in Ref. 1, and we reproduce those results in Fig. 1. The figure shows the growth rate normalized to low hybrid frequency $\omega_{LH} = \omega_{ce}\sqrt{m/M}$ as a function of a Pierce parameter $\alpha = \omega_{LH}L/v_{0d}$ with $v_{0d} = v_0(L)$ being the equilibrium ion outflow velocity. The initial equilibrium ion velocity value was chosen as in Ref. 1, $v_{00} = 0.2\ v_{0d}$. Growth rate

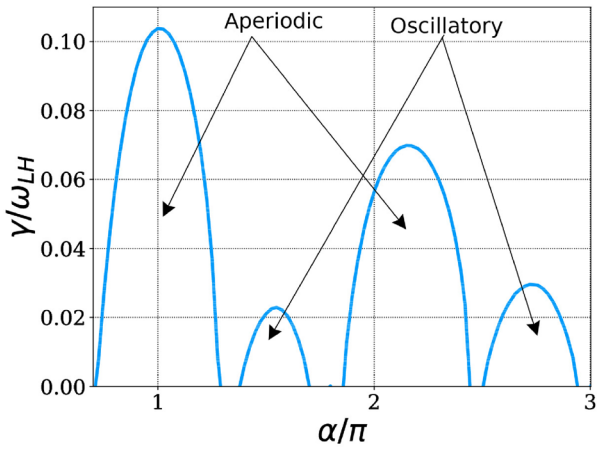

FIG. 1. Growth rate dependence on the Pierce parameter $\alpha = \omega_{LH}L/v_{0d}$ with initial ion velocity $v_{00} = 0.2v_{0d}$.

values were benchmarked with Table 1 in Ref. 1 and differ with those results by no more than 3%. Notice that values in Table 1 in Ref. 1 are obtained for different normalization processes, and therefore, to recover them, one needs to multiply γ/ω_{LH} by α.

As was shown in Ref. 1, the discussed model has only two external parameters: α and $q = 1 - (v_{00}/v_{0d})^2$. Here, we use v_{00}/v_{0d} instead of q.

Figure 1 shows four Pierce instabilities zones.[6] For $\alpha < 0.7\ \pi$, the plasma is stable, while for large α, more zones will appear. Each odd zone (counting starts from the small α) has aperiodic instability $Re(\omega) = 0$, while even zones have oscillatory instabilities $Re(\omega) \neq 0$. For example, Fig. 1 shows two aperiodic zones for $\alpha \sim \pi$ and $\alpha \sim 2.2\pi$ and two oscillatory zones $\alpha \sim 1.5\pi$ and $\alpha \sim 2.7\pi$. The zone number also defines the number of zeros of the unstable eigenfunction, and therefore, higher zones correspond to higher effective wave-numbers. This means that to consider higher number zones, one needs to take into account small-scale effects such as finite Larmor radius effect or charge separation.

IV. NONLINEAR EVOLUTION

The main objective of this paper is to track a nonlinear evolution of the instability discussed in Sec. III. Therefore, the full system of Eqs. (1)–(7) was solved numerically. In order to track the stage of nonlinear evolution, we define energy-like functionals and follow their time evolution

$$E_n = E\left[\frac{n}{n_{00}}\right], \quad E_v = E\left[\frac{v}{v_{00}}\right],$$
$$E_\phi = E\left[\frac{e\phi}{Mv_{00}^2/2}\right], \quad \text{with} \quad E[f] = \sqrt{\frac{1}{L}\int_0^L dz|f(z)|^2}. \tag{11}$$

Time evolutions of energy-like functionals for aperiodic ($\alpha = 1.05\ \pi$) and oscillatory ($\alpha = 1.55\ \pi$) Pierce zones are shown in Fig. 2. The evolution for both zones clearly shows the linear growth phase with transition into nonlinear saturation.

A. The aperiodic instability zone

In the aperiodic zone, for sufficiently small initial conditions, the unstable eigenfunction starts growing exponentially in time. The linear growth phase corresponds to the time $t\omega_{LH} < 100$ in Fig. 2(a). The shape of the unstable eigenfunction in the first Pierce zone is shown in Fig. 3(a) where the initial Gaussian profile (blue solid line) transforms into eigenfunction and starts to grow exponentially in time. After some time, when $n \sim n_0$, the nonlinear effects start to slow down the linear growth. Eventually, the new stationary equilibrium is reached as shown in the time evolution plot of total density [Fig. 3(b)]. The blue dashed line shows the initial density profile, and then, the red dotted line represents the evolution of density during the nonlinear regime which is a combination of large density perturbation and equilibrium density. After about $t\omega_{LH} \sim 105$, the new equilibrium profile is formed, and it stays constant for the rest of the simulation $105 < t\omega_{LH} < 500$, as shown by green and purple solid lines for times $t\omega_{LH} = 105$ and $t\omega_{LH} = 500$, respectively, which coincide.

It is interesting to note that new density equilibrium forms a prominent peak in the beginning of the acceleration region whose origin is the form of the unstable density eigenfunction shown in Fig. 3(a). Therefore, the continuity equation

$$(n_0 + n)(v_0 + v) = const$$

implies that the total velocity will have the deceleration region in the new equilibrium as shown in Fig. 3(c). The perturbation of electrostatic potential corresponding to the described density and velocity profiles is shown in Fig. 3(d). The perturbation is plotted rather than a full value of

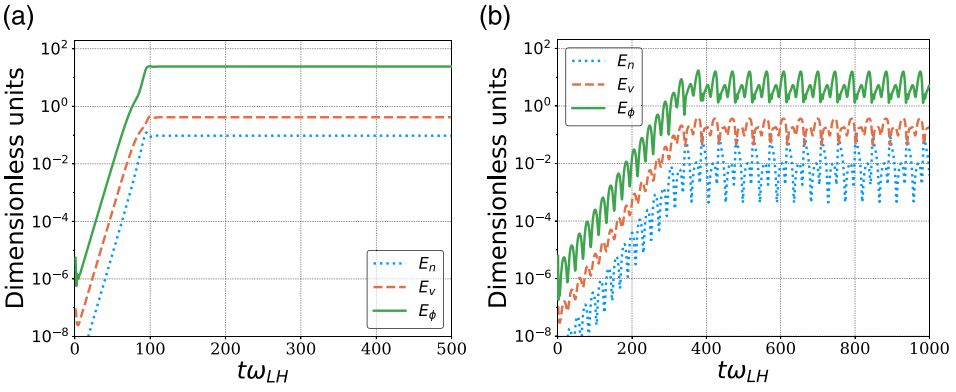

FIG. 2. Time evolution of functionals (11) with initial ion velocity $v_{00} = 0.2\ v_{0d}$. (a) Aperiodic zone with $\alpha = 1.05\ \pi$ and (b) oscillatory zone with $\alpha = 1.55\ \pi$.

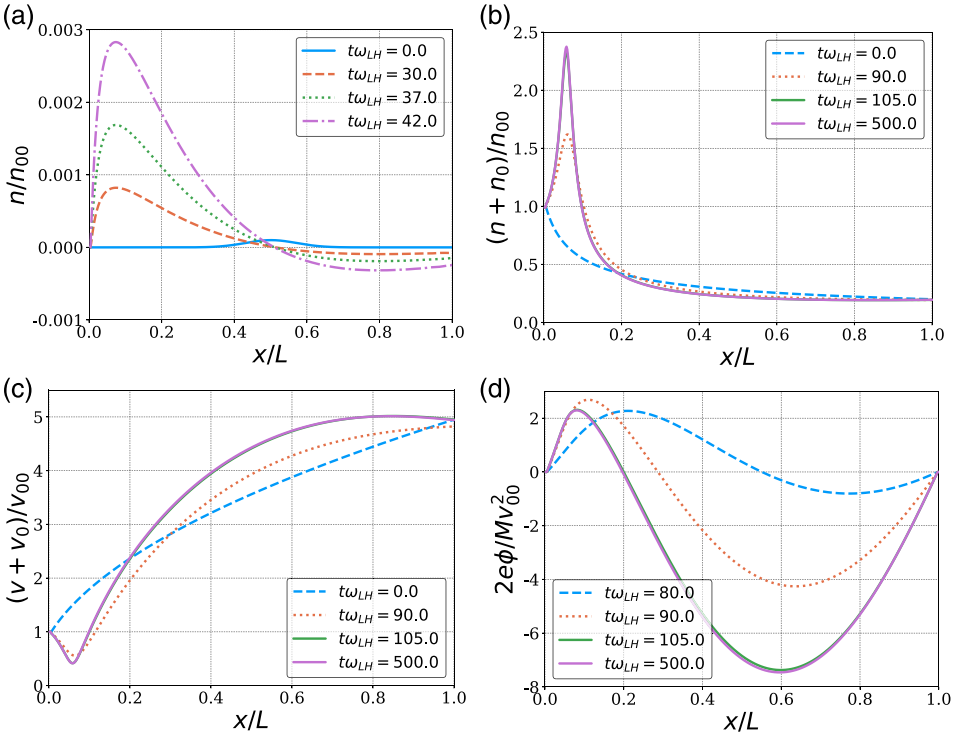

FIG. 3. The time evolution of ion density, ion velocity, and electrostatic potential spatial profiles in the aperiodic Pierce zone for $\alpha = 1.05\ \pi$ and initial ion velocity $v_{00} = 0.2\ v_{0d}$. (a) Density perturbation, (b) full density, (c) full ion velocity, and (d) electrostatic potential perturbation.

electrostatic potential, as the perturbation is still relatively small in comparison to the equilibrium value, which is

$$\frac{2e\phi_0}{Mv_{00}^2} = \left(1 - \left(\frac{v_{0d}}{v_{00}}\right)^2\right)\frac{x}{L}. \tag{12}$$

B. The oscillatory instability zone

In the oscillatory zone, the situation is similar, but the growth rate is smaller than in the preceding aperiodic zone, and so, the linear phase is longer $t\omega_{LH} < 350$. At the linear phase, the eigenfunction grows exponentially in time and additionally oscillates as shown in Fig. 4. Every figure in this subsection is branched into two sub-figures for the first and second half of the oscillation period. In the nonlinear regime, the new stationary equilibrium is replaced with a standing wave. Figure 5 shows a standing density wave which is similar to aperiodic solution shown in Fig. 3(b) but oscillates in time. Similar standing waves can be observed for velocity in Fig. 6 and electrostatic potential perturbation in Fig. 7.

The natural question arises if solutions found in Secs. IV A and IV B are stable. In order to confirm it, we have performed numerical simulations where new stationary/standing wave solutions in the first two Pierce zones were perturbed with relatively large arbitrary perturbations $\delta n \sim n$. It was verified that the perturbation damps away with time, and the found equilibria are again recovered.

V. FINITE LARMOR RADIUS EFFECTS

As was mentioned earlier, the Pierce zone number defines the number of zeros of the unstable eigenfunction. For example, the unstable eigenfunction in the first Pierce zone has one zero in the interior region (excluding boundary points) as shown in Fig. 3(a), while the second Pierce zone has two as shown in Fig. 4. Therefore, the effective wavelength decreases with a larger zone number. In this situation, one needs to include effects relevant to smaller scales. The next order term is the finite Larmor radius (FLR) effect,[5] which modifies the electron equation (6) as

$$\partial_x^2\phi + \frac{1}{n_0}\partial_x n_0 \partial_x \phi + \frac{m\omega_{ce}^2}{en_0}\left(n - \rho_e^2\partial_x^2 n\right) = 0, \tag{13}$$

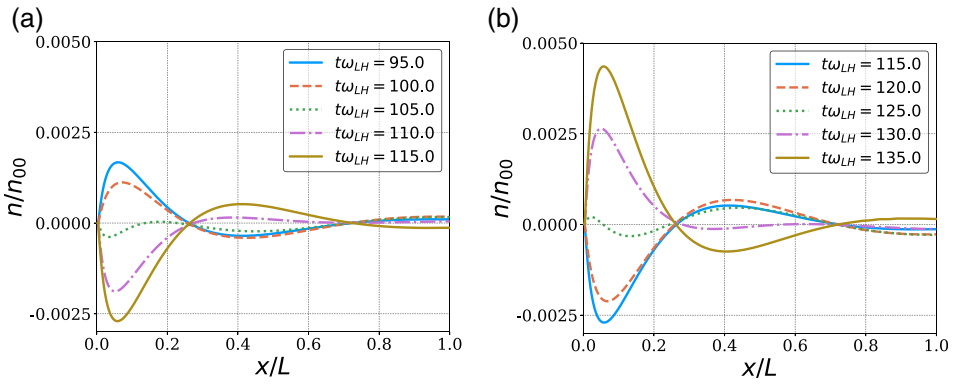

FIG. 4. Linear growth of unstable eigenfunction in the oscillatory Pierce zone for $\alpha = 1.55\pi$ and initial ion velocity $v_{00} = 0.2\ v_{0d}$. (a) First half period of oscillation and (b) second half period of oscillation.

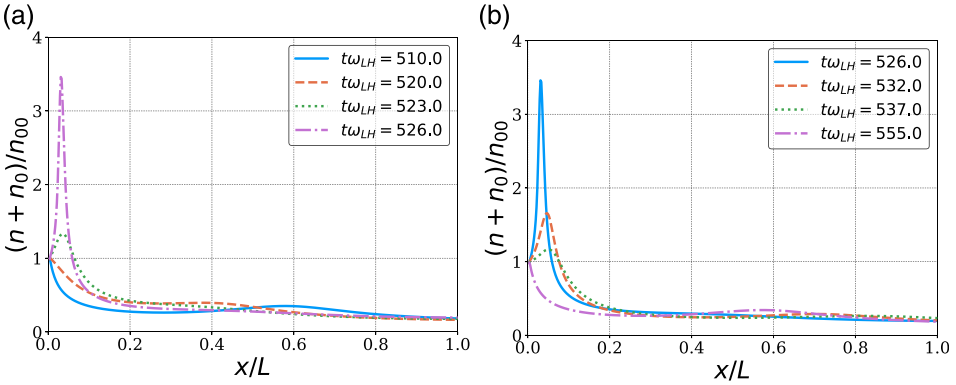

FIG. 5. Oscillating quasi-stationary profile of ion density in the oscillatory Pierce zone for $\alpha = 1.55\pi$ and initial ion velocity $v_{00} = 0.2\ v_{0d}$. (a) First half period of oscillation and (b) second half period of oscillation.

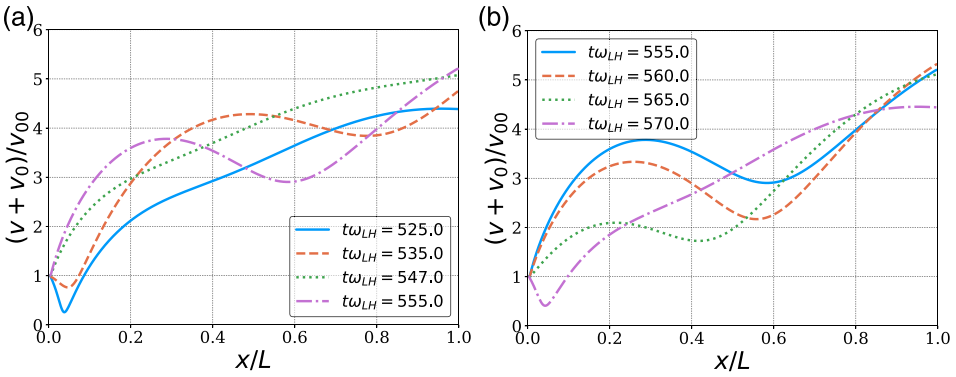

FIG. 6. Oscillating quasi-stationary profile of ion velocity in the oscillatory Pierce zone for $\alpha = 1.55\pi$ and initial ion velocity $v_{00} = 0.2\ v_{0d}$. (a) First half period of oscillation and (b) second half period of oscillation.

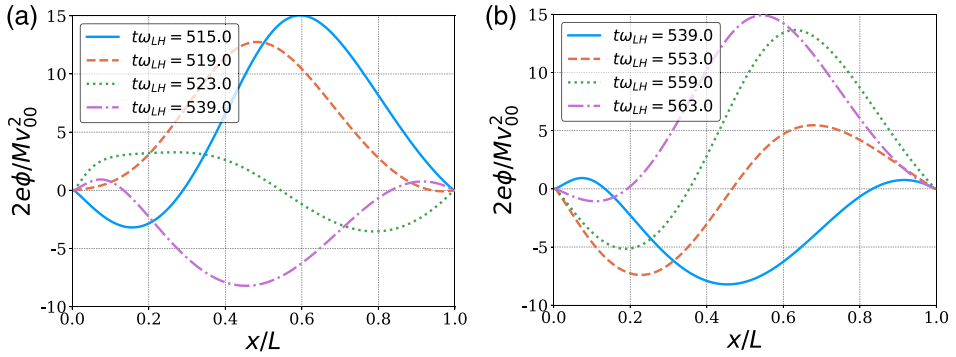

FIG. 7. Oscillating quasi-stationary profile of electrostatic potential perturbation in the oscillatory Pierce zone for $\alpha = 1.55\pi$ and initial ion velocity $v_{00} = 0.2\ v_{0d}$. (a) First half period of oscillation and (b) second half period of oscillation.

where ρ_e is an electron Larmor radius. The procedure to derive this equation (i.e., perturbative expansion in the limit of strong magnetic field $\partial_t \ll \omega_{ce}$) can be found in Ref. 5.

The new free parameter in Eq. (13), electron Larmor radius, is chosen to be $\rho_e = 0.05L$ in dimensionless units, which corresponds to typical Hall thruster acceleration region length $L \sim 1$ cm, electron temperature $T_e = 15$ eV, and magnetic field $B = 160$ G.

Numerical simulation results for linear growth rates with FLR effects are shown in Fig. 8(a). One can see that FLR effects stabilize higher order zones, while the first zone remains almost without modifications. If one investigates the

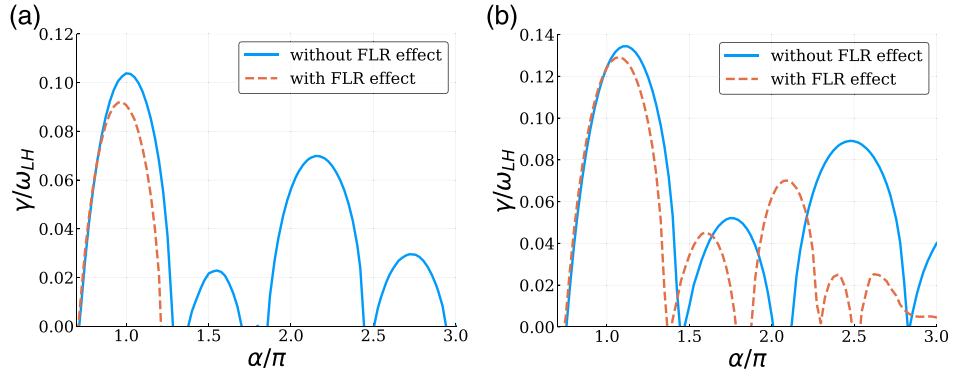

FIG. 8. Effect of FLR on the linear growth rate, for $L/\rho_e = 20$. (a) $v_{00} = 0.2v_{0d}$ (instability was absent for $\alpha > 1.21\ \pi$) and (b) $v_{00} = 0.4v_{0d}$.

parameter space further, higher Pierce zones may be stabilized partially as it is shown in Fig. 8(b) where the $v_{00}/v_{0d} = 0.4$ parameter was used. Nonlinear simulations reveal that dynamics is not significantly modified by FLR effects.

VI. CONCLUSIONS

In this paper, we have investigated the linear and nonlinear regimes of the nonlocal instability of axial lower-hybrid modes in a plasma with the ion flow. The reactive linear instability occurs as a result of the interaction of negative and positive energy modes in plasmas with the ion flow. The mode coupling occurs via the boundary conditions. The linear theory of the instability first described in Ref. 1 has been confirmed here with initial value numerical simulations and thus provided the necessary linear benchmark for our nonlinear studies.

The instability growth rate and the form of unstable eigenfunction which depend on the Pierce parameter α are shown in Fig. 1 where one can see distinct Pierce zones (which is in full agreement with the results obtained in Ref. 1). The effective wave number of the eigenfunction grows with a zone number. We find a significant modification of previous linear results[1] with the addition of finite Larmor radius effects which are significant in the case of short wavelengths. As shown in Fig. 8, the first Pierce zone stays relatively unchanged, while higher order zones are stabilized.

We have found that, after the initial linear growth phase, the aperiodically unstable mode saturates into a new nonlinear equilibrium which is shown in Fig. 3. The interesting feature of this equilibrium is the presence of the deceleration zone as shown in Fig. 3(c). The deceleration zone can be related to the shape of the unstable density eigenfunction which has a maximum at this location (respectively, the velocity eigenfunction has a minimum at the same location). It is of interest to note that somewhat similar non-monotonous electric field profiles (that include deceleration regions) were observed in experiments.[16,17] In the oscillatory zone, the oscillatory eigenfunction in the nonlinear regime becomes the standing wave with similar spatial features but oscillating in time.

The classical Pierce problem (in our case $v_{00} = v_{0d}$) has similar solutions, i.e., stationary and oscillating nonlinear equilibria, as was investigated by many authors, most notably by Godfrey.[18] Previous works have identified the regimes when oscillating solutions bifurcate (at some values of Pierce parameter α) into the combination of oscillating modes, leading to the chaotic oscillations.[18–20] We did not find such bifurcations or chaotic solutions in the first four Pierce zones in our case. We have investigated the stability of the new equilibrium state and found that it is stable. An important difference between the standard Pierce modes as in Ref. 6 and our case is that our profile of the ion velocity is nonuniform, resulting in partial suppression of the instability for higher zones. We conjecture that partial mode stabilization and the shift of Pierce zones for non-uniform profiles relative to the Pierce instability are the reasons for the absence of chaotic regimes. Further parametric studies with respect to α, v_{00}/v_{0d} parameters, and initial conditions to support this claim are left for future work.

In this paper, we neglect all resistive effects, and so, the axial instability discussed in Ref. 11 does not occur here. For some typical plasma parameters though, the growth rates of both instabilities can be of the same order, $\gamma \sim 0.1\omega_{LH}$. We note here that the nonlinear stages for the resistive mode of Ref. 11 and for the nonlocal (Pierce like) mode studied here are different. In the first case, where instability is driven by resistive electron cross-field current, the instability is local. In this case, local nonlinear interactions due to ion trapping[21] are the saturation mechanism which results in wave sharpening and breaking, leading to cnoidal type waves. For the nonlocal instability induced by boundary effects, only selected mode(s) continue to grow seemingly, excluding the growth (generation) of the shorter wavelengths. The nonlinear effects saturate the mode by modifying the instability source—the velocity flow profile, thus resulting in a velocity profile which has a local minimum.

It would be important to investigate the interaction of the resistive (local) modes, as in Ref. 11, with global modes as studied here. Other effects which are omitted here are plasma density gradients which can also destabilize the azimuthal lower-hybrid mode.[5,22] The interaction of axial modes (due to resistive and boundary effects) with azimuthal modes will have to be investigated within a unified framework which is left for future studies.

ACKNOWLEDGMENTS

This work was supported in part by NSERC, Canada, and the U.S. Air Force Office of Scientific Research under Award Nos. FA9550-15-1-0226 and FA9550-18-1-0132.

[1]A. Kapulkin and E. Behar, "Ion beam instability in Hall thrusters," IEEE Trans. Plasma Sci. **43**, 64 (2015).
[2]A. Smirnov, Y. Raitses, and N. J. Fisch, "Experimental and theoretical studies of cylindrical Hall thrusters," Phys. Plasmas **14**(5), 057106 (2007).
[3]T. Ito, C. V. Young, and M. A. Cappelli, "Self-organization in planar magnetron microdischarge plasmas," Appl. Phys. Lett. **106**(25), 254104 (2015).
[4]A. B. Mikhailovskii, *Theory of Plasma Instabilities, Vol. 1: Instabilities of a Homogeneous Plasma* (Springer, New York, 1974).
[5]A. I. Smolyakov, O. Chapurin, W. Frias, O. Koshkarov, I. Romadanov, T. Tang, M. Umansky, Y. Raitses, I. D. Kaganovich, and V. P. Lakhin, "Fluid theory and simulations of instabilities, turbulent transport and coherent structures in partially-magnetized plasmas of E × B discharges," Plasma Phys. Controlled Fusion **59**, 014041 (2017).
[6]J. R. Pierce, "Limiting stable current in electron beams in the presence of ions," J. Appl. Phys. **15**, 721 (1944).
[7]O. Koshkarov, A. I. Smolyakov, I. D. Kaganovich, and V. I. Ilgisonis, "Ion sound instability driven by the ion flows," Phys. Plasmas **22**, 052113 (2015).
[8]T. Klinger, F. Greiner, A. Rohde, A. Piel, and M. E. Koepke, "Van der Pol behavior of relaxation oscillations in a periodically driven thermionic discharge," Phys. Rev. E **52**, 4316–4327 (1995).
[9]C. Rapson, O. Grulke, K. Matyash, and T. Klinger, "The effects of boundaries on the ion acoustic beam-plasma instability in experiment and simulations," Phys. Plasmas **21**, 052103 (2014).
[10]V. I. Kuznetzov and A. Y. Ender, "Stability theory of Knudsen plasma diodes," Plasma Phys. Rep. **41**, 905–917 (2015).
[11]O. Koshkarov, A. I. Smolyakov, I. V. Romadanov, O. Chapurin, M. V. Umansky, Y. Raitses, and I. D. Kaganovich, "Current flow instability and nonlinear structures in dissipative two-fluid plasmas," Phys. Plasmas **25**, 011604 (2018).

[12]S. Chable and F. Rogier, "Numerical investigation and modeling of stationary plasma thruster low frequency oscillations," Phys. Plasmas **12**, 033504 (2005).
[13]J. P. Boeuf and L. Garrigues, "Low frequency oscillations in a stationary plasma thruster," J. Appl. Phys. **84**, 3541 (1998).
[14]S. Barral and E. Ahedo, "Low-frequency model of breathing oscillations in Hall discharges," Phys. Rev. E **79**, 046401 (2009).
[15]B. D. Dudson, M. V. Umansky, X. Q. Xu, P. B. Snyder, and H. R. Wilson, "BOUT++: A framework for parallel plasma fluid simulations," Comput. Phys. Commun. **180**, 1467 (2009).
[16]J. Vaudolon, B. Khiar, and S. Mazouffre, "Time evolution of the electric field in a Hall thruster," Plasma Sources Sci. Technol. **23**, 022002 (2014).
[17]J. Vaudolon and S. Mazouffre, "Observation of high-frequency ion instabilities in a cross-field plasma," Plasma Sources Sci. Technol. **24**, 032003 (2015).
[18]B. B. Godfrey, "Oscillatory nonlinear electron flow in a pierce diode," Phys. Fluids **30**(5), 1553–1560 (1987).
[19]H. Matsumoto, H. Yokoyama, and D. Summers, "Computer simulations of the chaotic dynamics of the pierce beam–plasma system," Phys. Plasmas **3**(1), 177–191 (1996).
[20]S. Kuhn, "The physics of bounded plasma systems (BPS's): Simulation and interpretation," Contrib. Plasma Phys. **34**(4), 495–538 (1994).
[21]R. C. Davidson, *Methods in Nonlinear Plasma Theory* (Academic Press, New York, 2012).
[22]A. A. Litvak and N. J. Fisch, "Resistive instabilities in Hall current plasma discharge," Phys. Plasmas **8**, 648 (2001).